



## REDUCING THE HEAT LOSS AT NIGHT FROM SOLAR WATER HEATERS OF THE INTEGRATED COLLECTOR-STORAGE VARIETY

DAVID FAIMAN<sup>\*,\*\*,\dagger</sup>, HAIM HAZAN<sup>\*\*\*</sup> and IDO LAUFER<sup>\*\*\*\*</sup>

<sup>\*</sup>Department of Solar Energy and Environmental Physics, Jacob Blaustein Institute for Desert Research, Ben-Gurion University of the Negev, Sede Boqer Campus, 84990 Israel

<sup>\*\*</sup>Department of Physics, Ben-Gurion University of the Negev, Beer Sheva, 84105 Israel

<sup>\*\*\*</sup>Negev Soltech Ltd, Temed Industrial Park, D.N. Aravah, 86800 Israel

<sup>\*\*\*\*</sup>Department of Chemical Engineering, Ben-Gurion University of the Negev, Beer Sheva, 84105 Israel

Received 23 August 2000; revised version accepted 22 January 2001

Communicated by DOUG HITTLE

**Abstract**—Experimental data and an analysis are presented for a solar water heater of the integrated collector-storage variety. The novelty of the particular unit investigated lies in the fact that its design incorporates a device that automatically lowers the heat-loss coefficient of the system during night time. This overcomes one of the basic problems associated with solar water heaters of this kind. The analytical apparatus employed for the study is our previously-published MUE method but with the incorporation of some newly suggested experimental details that lead to improved accuracy. © 2001 Elsevier Science Ltd. All rights reserved.

### 1. INTRODUCTION

A major performance difference between solar water heaters which employ separate components for heating and storage, and those which integrate these two functions into a single unit, is their night time heat loss properties.

Typical systems which separate the functions of heating and storage employ flat plate collectors to allow solar radiation to heat the water during daytime, when ambient temperatures are comparatively high relative to those at night. The solar heated water is then transferred to an insulated storage tank which would have a UA value considerably lower than that of the solar collector. In such circumstances, hot water in storage at the end of a day would retain a substantial part of its energy for use the next morning.

On the other hand, if the collector-storage system is a single unit, then, however well insulated the rear and sides of the storage tank might be, its solar collecting face would constitute a significant source of night time heat loss. As a result, the water temperature would drop by considerable amounts overnight, often leaving little, if any, useful energy the next morning.

In order to help quantify the problem, consider a cylindrical storage tank of nominal volume 100 l. Typical internal dimensions might be 0.44 m diameter and 0.66 m length. Let us suppose that the tank is enveloped in a 0.05-m thickness layer of glass wool insulation,  $k = 0.037 \text{ W m}^{-1} \text{ K}^{-1}$  (Kreith and Bohn, 1986). The total surface area for heat loss is  $1.22 \text{ m}^2$ , hence the total heat loss coefficient of the insulated tank will be  $UA = 0.90 \text{ W K}^{-1}$ .

If the water in such a tank had reached, say,  $60^\circ\text{C}$  by sunset on a given day, and the mean ambient overnight temperature was  $10^\circ\text{C}$ , then it is a simple calculation to determine that by sunrise the next morning (typically 12 h later) the temperature of the water in the tank would still be above  $55^\circ\text{C}$ .

On the other hand, a single-unit collector-storage system would need to have one surface of the storage tank — namely the solar collecting surface — relatively ‘exposed’ to the nocturnal ambient conditions. Since the effective UA value of that surface would typically be, say,  $5 \text{ W K}^{-1}$ , one may calculate that the final tank temperature would have dropped to below  $40^\circ\text{C}$  by the next morning.

The purpose of the present paper is to present a practical method for reducing the nocturnal heat loss in an integrated collector-storage solar water heater and to demonstrate, quantitatively, its

<sup>\dagger</sup>Author to whom correspondence should be addressed.  
Tel.: +972-8-659-6933; fax: +972-8-659-6736;  
e-mail: faiman@bgumail.bgu.ac.il



Fig. 1. The SOLTECH 1000™ integrated collector–storage solar water heater under study.

effectiveness in the case of an actual pre-production commercial unit.

## 2. REDUCING THE NIGHT TIME HEAT LOSS COEFFICIENT

The basic problem that must be overcome in order to improve the night time heat storage properties of an integrated collector–storage solar water heater is that a means must be found to change the night time heat loss coefficient of the collector aperture area. In the case of the unit discussed in the present study, a SOLTECH 1000™ (Fig. 1), the storage tank is designed in the following manner (Hazan, 2000). One of its walls is coated on its outer surface (i.e. beneath the glazing, the existence of which goes without saying) so as to enable it to act as a solar absorber plate. Beneath that surface, and parallel to it, is a plate made of insulated material, positioned so as to permit thermosiphon flow of a sheet of water between the two planes during the day. At night (more specifically, at the onset of reverse-ther-

mosiphon flow), a mechanical valve closes in order to prevent movement of the sheet of water between the above-described absorber and insulated planes. Fig. 2 shows a schematic vertical cross-section through the unit in order to clarify these ideas. It is this layer of stagnant water, together with its underlying insulated support plane which effectively reduce the night time heat loss coefficient of the collector aperture compared to its day time value.

We now describe the experiments that were performed in order to measure these two heat loss coefficients and, at the same time, to determine all parameters necessary for predicting the performance of this solar water heater under various climatic conditions.

## 3. EXPERIMENTAL METHODOLOGY

The solar water heater under study is basically a ‘flat-plate’ solar collector, of aperture area  $1.15 \text{ m}^2$ , but with a built-in storage capacity of 120 l. Because of the large thermal mass of such a body of water, the system can never achieve thermodynamic steady state conditions and hence, standard test methods for flat plate solar collectors are inapplicable. However, some years ago, cognizant of the need for a simple but accurate test method for integrated collector–storage systems of this kind, we developed the MUE test method (Faiman, 1984). In that paper we showed that the ‘maximum useful efficiency’ (MUE) of such a system can be cast in a mathematical form which is similar to the familiar Hottel–Whillier–Bliss equation (Bliss, 1959) for a low-mass flat-plate collector, but where the variables take on time-averaged values. Specifically (Faiman, 1984),

$$\mu = \bar{K} F_E \eta_o - \frac{F_E U_L (\bar{T} - \bar{T}_a)}{\bar{I}} \quad (1)$$

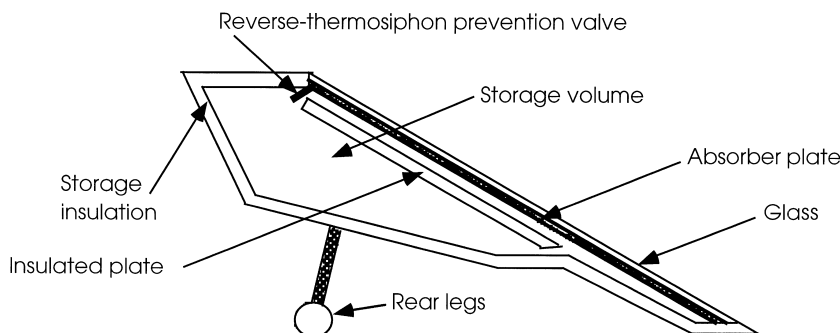


Fig. 2. Schematic vertical cross-section through the system in order to illustrate the function of the reverse-thermosiphon prevention valve, and the insulated plate which isolates the bulk of the stored heat from the stagnant water layer trapped, at night, beneath the absorber plate.

In Eq. (1),  $T$  is the temperature of the water in storage,  $T_a$  is the ambient temperature and  $I$  is the irradiance on the aperture plane of the collector.  $\eta_o$  is the optical efficiency and  $U_L$  the heat loss coefficient of the collector–storage unit.  $K$  is the incidence angle modifier and  $F_E$  is an enthalpy retrieval factor defined as:

$$F_E = \frac{M_w C_w}{M_w C_w + M_{CS} C_{CS}} \quad (2)$$

where  $M_w$  and  $C_w$  are, respectively, the mass and heat capacity of the water and  $M_{CS}$  and  $C_{CS}$  are the respective mass and heat capacity of the material from which the collector–storage unit is fabricated. Most important of all, the bars indicate time average over the daily heating period, from sunrise until the time the water reaches its maximum daily temperature — typically about 10 h. That is to say, we use *daily average*, rather than instantaneous, values of the variables in Eq. (1). The bar over  $K$  indicates a daily energy average, which is fairly constant on a monthly basis (Faiman, 1984). MUE is defined as:

$$\mu = \frac{M_w C_w (T_{\max} - T_{\text{sunrise}})}{A_c \int I(t) dt}$$

where  $A_c$  is the collector aperture area, and the integral is taken over the time from sunrise until the water reaches its maximum temperature.

We remark that, in contrast to a semi-empirical test method that was subsequently developed for testing integrated collector–storage systems (Bourges et al., 1991a,b), the MUE method is *not empirical*, in that all of its parameters have a clear physics-based interpretation. It follows directly from the fundamental heat flow equation, as a consequence of the long relaxation time of the system (Faiman, 1984). Since the principal purpose of the present study is to measure the difference between the day time and night time heat loss coefficients of the system, we shall adopt the MUE method owing to its greater suitability for this purpose.

The experimental measurements were made in much the manner that was previously described (Faiman, 1984), but with some improved techniques regarding achievable accuracy.

1. The need to stir the water before temperature measurements was overcome in the following manner. A rigid wooden rod was positioned so that its lowest end rested at the lowest point of the storage tank. Ten-litre amounts of water were then introduced into the tank and the

water levels were marked off on the rod. Six thermocouples were then attached to the rod in a manner such that they sampled the temperatures of successive 20-l volumes, at the (linear) mid-point of each 20-l volume, as indicated by the rod markings. Because of the unknown internal geometry of the storage tank, a number of experiments were then performed in order to determine the extent to which a true average water temperature could be calculated from the six thermocouple readings. Specifically, at the end of each of several heating periods, the average temperature was first calculated and the result then compared to the temperature achieved after vigorous stirring of the tank contents. Since the results of these comparisons differed by, at most, a fraction of 1°C, the simple (i.e. non-weighted) average value of the temperatures indicated by the six thermocouples was deemed an accurate enough estimate of the true average temperature of the water in the storage tank. The great advantage of not having to stir the water lies in the fact that a data logger could be employed to monitor all temperatures on a continuous basis.

2. The slope of the MUE graph illustrated in our previously published work (Faiman, 1984) had a relatively large experimental uncertainty owing to the combined natural scatter of the measured points and the fact that nature presented us with a relatively restricted range of temperatures. The reader is reminded that our experimental technique at that time was to allow the system to heat up by day and cool down at night and record the succession of daily maximum and minimum water temperatures. In such circumstances, similar temperature ranges tended to recur many times. In the present work, ice was added to the water on some evenings, in order to bring the starting temperature down close to 0°C. This, together with some exceptionally sunny spring days, produced an extended range of  $(T_{\max} - T_{\text{sunrise}})$  values and a correspondingly more linear MUE graph with relatively little scatter.

3. The importance of a MUE graph with low scatter lies in the fact that its slope represents an accurate measure of the day time heat loss coefficient of the collector–storage unit. The night time heat loss coefficient — which we wished to compare with the former — could be determined from the evening-to-morning heat losses recorded by the data logger.

In our previous work (Faiman, 1984) the nocturnal heat loss coefficient was used as a

confirmation of the slope of the MUE graph determined by day time measurements. That was a reasonable procedure since no special steps had been taken by the manufacturer of the unit under study at that time to provide any kind of night time insulation. In the present situation, it is the difference between the night time and day time heat loss coefficients that must serve as a measure of successful, or otherwise, system design.

We remark that solar irradiance was measured with a LiCor solid state ‘pyranometer’ positioned in the plane of the aperture. This sensor was calibrated, using the normal incidence method (Faiman *et al.*, 1992), relative to a secondary standard Eppley PSP black body pyranometer, the calibration of which is directly traceable to WMO reference instruments at Davos, Switzerland.

#### 4. RESULTS

##### 4.1. Night time heat loss coefficient

Ambient temperature and temperatures in the storage tank were continuously monitored (together with plane-of-aperture irradiance) during the period April 20–May 18, 1999. Because of the relatively slow response time of the water, it was deemed sufficient to record 1/2-h averages.

In order to compute the night time heat loss coefficient, we used data between 21:30 h at night and 04:00 h the following morning (Israel Standard Time). For each half hour of data, we calculated the difference between the mean water temperature and ambient, and then averaged the results over the  $\Delta t = 8.5$  h time period. This average,  $\langle T - T_a \rangle$ , was then divided into the temperature difference,  $(T_i - T_f)$ , between the water’s initial temperature and final temperature during this time period and the resulting quotient, up to a numerical constant, gives the required heat loss coefficient  $U_L A$ . Specifically:

$$U_L A = \frac{(M_w C_w + M_{CS} C_{CS})(T_i - T_f)}{\Delta t \langle T - T_a \rangle}. \quad (4)$$

The input data to Eq. (4) (actually,  $F_E U_L A$ ), are given in Table 1 for 23 days out of the stated 29-day period. The data not shown represent 6 nights during which the water temperatures were disturbed by the addition of ice to the system.

The night time heat loss coefficients calculated in Table 1 reveal two anomalous numbers, indicated in bold print. Apart from these (which we shall return to later), the remaining nightly values are in very good agreement with one another. Their mean and standard deviation are

Table 1. Input data for night time heat loss coefficient<sup>a</sup>

Date	$T_i$ (°C)	$(T_i - T_f)$ (°C)	$\langle T - T_a \rangle$ (°C)	$\Delta t$ (h)	$F_E U_L A$ (W K <sup>-1</sup> )
Apr 20, 99	45.3	4.8	27.6	8.5	2.84
Apr 21, 99	53.3	12.6	31.4	8.5	<b>6.61</b>
Apr 22, 99	<sup>b</sup>				
Apr 23, 99	43.7	4.3	26.5	8.5	2.68
Apr 24, 99	52.3	5.5	33.8	8.5	2.66
Apr 25, 99	59.2	6.6	39.4	8.5	2.76
Apr 26, 99	57.5	6.2	37.2	8.5	2.71
Apr 27, 99	60.9	6.8	40.3	8.5	2.76
Apr 28, 99	64.9	7.8	45.7	8.5	2.80
Apr 29, 99	66.1	7.9	45.5	8.5	2.84
Apr 30, 99	66.7	8.0	45.8	8.5	2.88
May 01, 99	<sup>b</sup>				
May 02, 99	40.5	3.5	19.8	8.5	2.87
May 03, 99	57.6	5.8	32.4	8.5	2.94
May 04, 99	65.5	7.3	40.8	8.5	2.96
May 05, 99	66.5	7.4	42.1	8.5	2.90
May 06, 99	<sup>b</sup>				
May 07, 99	41.9	7.5	20.0	8.5	<b>6.17</b>
May 08, 99	53.7	5.8	33.3	8.5	2.86
May 09, 99	53.5	5.8	34.1	8.5	2.77
May 10, 99	60.2	7.0	40.0	8.5	2.88
May 11, 99	61.1	7.0	40.5	8.5	2.82
May 12, 99	<sup>b</sup>			8.5	
May 13, 99	41.8	4.1	23.4	8.5	2.86
May 14, 99	<sup>b</sup>				
May 15, 99	42.4	4.0	23.3	8.5	2.79
May 16, 99	56.6	6.1	35.7	8.5	2.82
May 17, 99	61.8	6.9	39.6	8.5	2.85
May 18, 99	<sup>b</sup>				

<sup>a</sup> Bold print highlights two anomalous events discussed in the text.

<sup>b</sup> Indicates that ice was added.

$2.82 \pm 0.08$  W K<sup>-1</sup>, i.e. with a 3% spread about the mean. Because of some uncertainty about the appropriate value of  $M_{CS} C_{CS}$  for the construction material we have included only the 120 l of tank water in the final column of Table 1. Hence the factor of  $F_E$  in the column heading. Normalizing the result to the 1.15 m<sup>2</sup> of aperture area, we end up with a night time heat loss coefficient of:

$$F_E U_L = 2.45 \mp 0.07 \text{ W m}^{-2} \text{ K}^{-1}. \quad (5)$$

Regarding the two anomalous values of heat loss coefficient indicated in Table 1, we believe that they occurred due to an erratic behavior of the mechanical valve which shuts off reverse thermosiphon flow at night. Support for this conclusion can be found below, in our analysis of the day time heat loss coefficient.

##### 4.2. The day time MUE curve

As explained in Section 3, we have adopted the MUE formalism (Faiman, 1984) for the determination of the day time thermal (and optical) properties of this integrated collector–storage unit. For this purpose, each day’s maximum useable *energy* is calculated by observing the

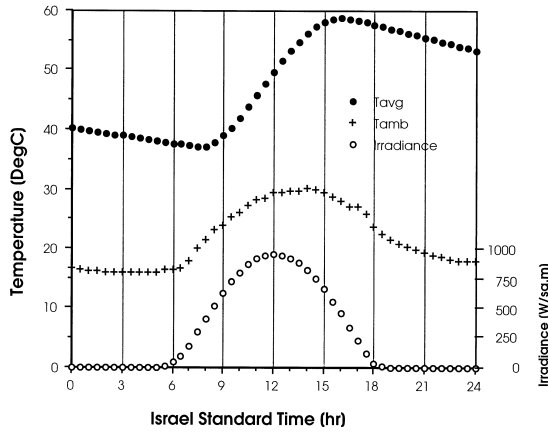


Fig. 3. Variation with time of water temperature  $T_{avg}$ , ambient temperature  $T_{amb}$ , and irradiance on the plane of aperture, for a typical day (May 16, 1999).

maximum average temperature achieved by the water in the storage tank and subtracting from it the temperature of the same water at sunrise. The difference is then multiplied by the heat capacity of the 120 l of water in storage. This clearly corresponds to the maximum useful energy that can be extracted from the system because if one were to wait longer, e.g. until sunset, the temperature of the water would decrease, as shown in

Fig. 3 for a typical day (May 16). Similarly, by dividing the maximum useful energy by the total irradiance received by the collector during the heating period, one arrives at the maximum useful efficiency. Again, this quotient is a maximum because it will decrease if we include solar energy received *after* the water temperature has reached its maximum. The daily values of MUE are then plotted against  $\langle T_{avg} - T_{amb} \rangle / \langle I \rangle$ , where  $T_{avg}$  and  $T_{amb}$  are, respectively, the average temperature of the water in the storage tank and the ambient temperature. This latter difference was calculated every half hour and averaged over the time from sunrise till maximum water temperature.  $\langle I \rangle$  is the average value of the irradiance on the aperture plane from sunrise until maximum water temperature. Table 2 shows the daily measured temperatures and the corresponding calculations for the MUE plot.

The results of this plot are shown in Fig. 4 for all days between April 20 through May 19, 1999. Apart from a single outlier (April 22), all points are seen to fall on a straight line (to within realistic estimated error bars of about  $\pm 10\%$ , coming mainly from variations in the calibration of the LiCor sensor) having a slope of  $-F_E U_L = -6.82 \text{ W m}^{-2} \text{ K}^{-1}$ .

Table 2. Day time measured data and calculated quantities for the MUE graph (Fig. 4)

Date	$\Delta t$ (h)	$T_{max}$ (°C)	$T_{sunrise}$ (°C)	$Q_{in}$ (kJ)	$\langle I \rangle$ ( $\text{W m}^{-2}$ )	$\langle T_{avg} - T_{amb} \rangle \equiv \Delta T$ (°C)	$\Delta T / \langle I \rangle$ ( $\text{W m}^{-2} \text{ K}^{-1}$ ) <sup>-1</sup>	MUE
Apr 20, 99	10.0	47.0	21.6	12,700	582	8.8	0.0151	0.527
Apr 21, 99	10.5	58.6	40.0	9330	602	25.4	0.0422	0.357
Apr 22, 99	9.5	48.7	39.7	4530	646	21.3	0.0330	0.179
Apr 23, 99	11.5	44.9	15.6	14,690	600	7.5	0.0125	0.514
Apr 24, 99	10.5	54.2	38.9	7680	541	23.5	0.0434	0.326
Apr 25, 99	10.5	61.7	46.2	7800	603	28.8	0.0478	0.298
Apr 26, 99	9.5	61.7	51.9	4890	529	32.1	0.0608	0.235
Apr 27, 99	10.5	63.5	50.7	6430	600	30.9	0.0515	0.246
Apr 28, 99	10.5	67.8	53.4	7240	648	34.8	0.0538	0.257
Apr 29, 99	10.5	69.2	56.2	6510	651	37.8	0.0580	0.230
Apr 30, 99	10.5	70.0	57.4	6310	634	37.0	0.0584	0.229
May 01, 99	10.5	69.5	57.8	5870	600	34.1	0.0568	0.225
May 02, 99	12.0	41.2	1.9	19,730	567	-6.7	-0.0118	0.700
May 03, 99	11.0	59.6	36.6	11,520	622	18.3	0.0294	0.407
May 04, 99	10.5	68.2	51.1	8540	628	28.1	0.0448	0.313
May 05, 99	10.5	69.6	57.3	6170	617	31.3	0.0507	0.230
May 06, 99	10.5	70.7	58.2	6260	614	34.6	0.0564	0.234
May 07, 99	12.5	43.5	7.8	17,900	555	-0.1	-0.0001	0.623
May 08, 99	11.0	55.7	33.6	11,050	579	18.5	0.0320	0.419
May 09, 99	11.0	56.3	47.3	4510	453	27.9	0.0617	0.219
May 10, 99	10.5	62.8	47.1	7890	622	29.3	0.0471	0.292
May 11, 99	10.5	63.9	52.4	5760	606	33.2	0.0547	0.219
May 12, 99	10.5	65.6	53.4	6140	607	34.6	0.0569	0.233
May 13, 99	11.5	42.8	7.4	17,740	591	0.2	0.0003	0.631
May 14, 99	11.0	59.3	37.3	11,030	614	20.6	0.0336	0.394
May 15, 99	11.5	43.4	6.7	18,430	599	-1.8	-0.0030	0.646
May 16, 99	11.0	58.7	38.1	10,340	608	21.1	0.0348	0.374
May 17, 99	11.0	64.1	49.8	7190	589	29.1	0.0494	0.268
May 18, 99	10.5	67.8	54.1	6860	608	32.1	0.0527	0.260
May 19, 99	11.5	43.5	8.6	17,510	571	-1.3	-0.0022	0.644

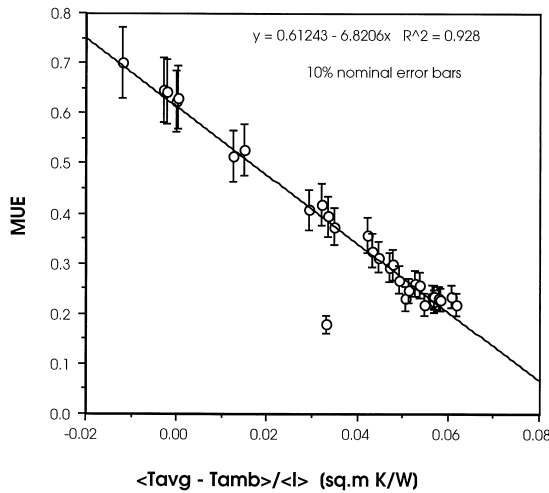


Fig. 4. MUE graph for SOLTECH 1000™ integrated collector-storage solar water heater under study.

## 5. DISCUSSION AND CONCLUSIONS

As regards the built-in mechanism (Hazan, 2000) for reducing the night time heat loss coefficient of the specific solar collector-storage system reported here, we find it to be successful in that it decreases the day time heat loss coefficient by a factor of nearly three. In practice, this means that if the water temperature had reached about 60°C at the end of a typical spring day's solar heating, then failure to use the water that night would result in a temperature drop of only 5°C, or thereabouts, by the next morning (see Fig. 3).

In Section 4.1 we speculated that on two occasions this mechanical reverse-thermosiphon valve appears not to have closed, in that on those occasions the night time losses were characteristic of a heat loss coefficient in excess of  $6 \text{ W m}^{-2} \text{ K}^{-1}$ . The basis of this speculation was the numerical similarity between this value and the slope of the (day time) MUE graph in Fig. 4. However, the small standard deviation ( $\pm 3\%$ ) among all other measured values of the night time heat loss coefficient ( $2.45 \text{ W m}^{-2} \text{ K}^{-1}$ ) lends credence to our interpretation of the two outliers as being truly anomalous, rather than part of a more widely spread distribution. Furthermore, the fact that there were only two such anomalies among a month of data indicates that such valve failures are comparatively isolated events. In fact, it is entirely possible that they were accidentally caused by our intervention during the course of these tests.

Turning now to the MUE method itself, one of its great virtues as a test method is that basically the same tank full of water is used on many successive nights in order to build up the efficiency graph. However, by the simple device of adding ice, as was done during the tests reported here, the MUE graph can be greatly extended (see Fig. 4), thereby, greatly increasing the accuracy of its slope value.

True, the MUE graph determines only the *maximum* useful energy that can be extracted from the system, but this is not necessarily an artificial number, and no more artificial than specifying any canonical draw pattern. Probably in a domestic context one would rarely extract this maximum. However, in an industrial context it would be a comparatively easy task to devise a sensor which empties the collector-storage unit when its maximum temperature is reached. After all, because of the long thermal relaxation time of such systems, it is easy to detect the maximum temperature since positive and negative water temperature fluctuations do not occur as they would in solar collectors with small time constants. As soon as the temperature begins to decrease, the maximum has been reached (see Fig. 3) and the system can then be emptied.

Finally, because the purpose of the present paper was to demonstrate the efficacy of a device (Hazan, 2000) that reduces the night time heat loss coefficient of an integrated collector-storage solar water heater, it has been sufficient to study the difference in day time and night time values of  $F_E U_L$ , arriving as we did at the values  $6.82 \text{ W m}^{-2} \text{ K}^{-1}$  during day time use and  $2.45 \pm 0.07 \text{ W m}^{-2} \text{ K}^{-1}$  during the night. For completeness, however, we remark that owing to the simple geometry of the solar collector part of the unit under study, its incidence angle modifier should be characteristic of typical flat-plate collectors (Rabl, 1985) and the value of  $F_E$ , if needed, may be simply calculated from a knowledge of the masses and material types of its component parts (Faiman, 1984).

## NOMENCLATURE

$A$	total system surface area, $\text{m}^2$
$A_c$	collector aperture area, $\text{m}^2$
$C_{cs}$	heat capacity of empty collector-storage unit, $\text{J kg}^{-1} \text{ K}^{-1}$
$C_w$	heat capacity of water, $\text{J kg}^{-1} \text{ K}^{-1}$
$F_E$	system enthalpy retrieval factor, -
$I$	solar irradiance on collector aperture, $\text{W m}^{-2}$

$k$	thermal conductivity of insulation, $\text{W m}^{-1} \text{K}^{-1}$
$K$	collector incidence angle modifier, –
$M_{\text{CS}}$	mass of empty collector–storage unit, kg
$M_{\text{W}}$	mass of water in storage, kg
$t$	time, s
$T$	temperature of water in storage, K
$T_{\text{a}}$	ambient temperature, K
$T_{\text{avg}}$	average value of $T$ , K
$T_{\text{f}}$	final night time temperature of water in storage, K
$T_{\text{i}}$	initial night time temperature of water in storage, K
$T_{\text{max}}$	maximum daily water temperature, K
$T_{\text{sunrise}}$	water temperature at sunrise, K
$U$	generic heat loss coefficient, $\text{W m}^{-2} \text{K}^{-1}$
$U_{\text{L}}$	system heat loss coefficient, $\text{W m}^{-2} \text{K}^{-1}$
$\eta_{\text{o}}$	collector optical efficiency, –
$\mu$	system maximum useful efficiency (MUE), –

*Acknowledgements*—One of the authors (I.L.) wishes to express his thanks to Professors Sydney Lang and Aharon Roy for several valuable discussions.

## REFERENCES

- Bliss R. W. (1959) The derivation of several ‘plate-efficiency factors’ useful in the design of flat-plate solar heat collectors. *Solar Energy* **3**, 55–64, and references therein.
- Bourges B., Rabl A., Leide B., Carvalho M. J. and Collares-Pereira M. (1991a) Accuracy of the European solar water heater test procedure. Part 1. *Solar Energy* **47**, 1–16.
- Bourges B., Rabl A., Leide B., Carvalho M. J. and Collares-Pereira M. (1991b) Accuracy of the European solar water heater test procedure. Part 2. *Solar Energy* **47**, 17–25, and references therein.
- Faiman D. (1984) Towards a standard method for determining the efficiency of integrated collector–storage solar water heaters. *Solar Energy* **33**, 459–463.
- Faiman D., Feuermann D. and Zemel A. (1992) Accurate field calibration of pyranometers. *Solar Energy* **49**, 489–492.
- Hazan H. (2000) *Israel Patent No. 118982* (other patents applied for).
- Kreith F. and Bohn M. S. (1986) In 4th edn, Principles of Heat Transfer, p. 647, Harper and Row, New York.
- Rabl A. (1985) In *Active Solar Collectors and Their Applications*, pp. 96–97, Oxford University Press, New York.